atmosphere

MDPI

Article

Characterization of the Elemental Composition of Aerosols Emitted in the Dry Season of the Pantanal Wetland, Brazil

Lucas Cardoso Ramos [1,*], Thais Costa Brunelli [1], Flávio César Vicentin [2], Leone Francisco Amorim Curado [1], André Matheus de Souza Lima [1], Fernando Gonçalves Morais [3], Rafael da Silva Palácios [4], Nicolas Neves de Oliveira [1] and João Basso Marques [1,*]

1 Graduate Program in Environmental Physics, Institute of Physics, Federal University of Mato Grosso (UFMT), Cuiabá 78060-900, MT, Brazil
2 National Synchrotron Light Laboratory (LNLS), National Center for Research in Energy and Materials (CNPEM), Campinas 13083-100, SP, Brazil
3 Institute of Physics, University de São Paulo (USP), São Paulo 05508-090, SP, Brazil
4 Institute of Geosciences, Federal University of Pará (UFPA), Belém 66075-110, PA, Brazil
* Correspondence: lucasramos@fisica.ufmt.br (L.C.R.); jbassofisico@gmail.com (J.B.M.)

Abstract: The Brazilian Pantanal region experiences intense biomass burning during the dry season, releasing large quantities of gasses and particles into the atmosphere, which have serious implications on both the climate system and public health. Understanding the dynamics of these emissions is crucial for mitigating the impact on the ecosystem, its functioning, and potential anthropogenic disturbances. This study focused on analyzing emissions in the northern Pantanal during the 2022 drought. Concentrations of fine particulate matter ($PM_{2.5}$), black carbon (BC), and 25 chemical elements were measured using gravimetry, reflectance analysis, and X-Ray fluorescence, respectively, from samples collected between August and October 2022. The average concentrations of $PM_{2.5}$ and BC increased approximately 4-fold and 2.5-fold, respectively, compared to averages from a decade ago. Significant increases were also observed in elements such as sulfur (S), potassium (K), iron (Fe), and silicon (Si). The maximum concentrations were comparable to values typical of the southern Amazon, a region known for high deforestation rates and land use changes. Elemental analysis revealed substantial shifts in concentrations, primarily associated with biomass burning (BB) and soil suspension. Additionally, enrichment factor (Ef) analysis showed that lead (Pb) levels, correlated with human activities, were 200 times higher than those found under clean atmospheric conditions.

Keywords: AOD; EDXRF; biomass burning; black carbon; soil suspension

Citation: Ramos, L.C.; Brunelli, T.C.; Vicentin, F.C.; Curado, L.F.A.; Lima, A.M.d.S.; Morais, F.G.; Palácios, R.d.S.; Oliveira, N.N.d.; Marques, J.B. Characterization of the Elemental Composition of Aerosols Emitted in the Dry Season of the Pantanal Wetland, Brazil. *Atmosphere* **2024**, *15*, 1361. https://doi.org/10.3390/atmos15111361

Academic Editors: Tariq Mehmood and Junjie Liu

Received: 23 September 2024
Revised: 28 October 2024
Accepted: 31 October 2024
Published: 13 November 2024

1. Introduction

Atmospheric aerosols are solid or liquid particles suspended in the atmosphere, ranging in size from approximately 0.001 to 100 μm. These particles play a critical role in the climate system, and their high spatial and temporal variability represents one of the greatest sources of uncertainty in Earth's radiative balance [1,2]. These uncertainties stem from a limited understanding of the physical and chemical properties of aerosols [3,4], which can affect the climate both directly by scattering and absorbing solar radiation [5,6] and indirectly by modifying cloud properties, thereby influencing precipitation efficiency [7,8] and atmospheric reflectance.

Certain aerosols, such as those containing carbon and mineral dust, have a high capacity to absorb radiation. Soot carbon particles, known as black carbon (BC), are emitted by biomass burning (BB), composed almost entirely of carbon, and significantly contribute to the absorption of solar radiation [9], influencing atmospheric stability [6]. BC emissions result from various combustion processes, including biomass burning. The aging process of BC alters its lifespan and removal rate, complicating our understanding of its true role in the climate system [7]. While aerosols generally have a cooling effect on the climate,

counteracting the impact of greenhouse gasses, BC exerts a direct radiative forcing, making it one of the key contributors to global warming [10].

In addition to the effects on the climate, emissions of particulate matter associated with climate change have directly impacted the health of the population in every region of the planet [11]. In Brazil, recent research has shown that biomass burning (BB) emissions significantly worsen hospital records related to respiratory diseases [12]. Local studies have also found a strong correlation between BB emissions and increased hospitalizations of children due to respiratory illnesses [13], moreover, the association between meteorological conditions and aerosols increases viral transmission and the risk of mortality from respiratory diseases [14,15].

In Brazil, several studies have characterized the physical and chemical properties of aerosols in the central Amazon [5,16–20]. However, studies are still scarce in the south of the Amazon basin [21]. This region, denominated as Pantanal Biome, is a unique ecosystem with peculiar characteristics due to flooding regimes, rich in biodiversity, and providing special conditions for monitoring the physical and chemical properties of aerosols. The Pantanal is an excellent laboratory for monitoring aerosols, as during the rainy season it can be representative of a practically clean atmosphere, under natural conditions. During the dry season, as in other areas of South America and Brazil, it is strongly influenced by emissions from biomass burning [22,23]. The concentrations of atmospheric aerosols in the Pantanal northern region increase in the dry season. This is attached to anthropogenic activities such as biomass burning, gold mining, and carriage [21].

The Pantanal is the largest contiguous wetland in the world [24,25]. Recent changes in land use and atmosphere conditions contributed greatly to the unprecedented forest fires recorded in the region, with approximately half of the area burned in 2020. This fire season was responsible for more than 3.9 million hectares burned with diverse impacts on the ecosystem, the hydrological cycle, and the economy [25–27]. The occurrence of the 2020 burning motivated this study, which aims to carry out a specific chemical characterization of BB emissions in the Pantanal, now using the 2022 drought as a reference. The chemical results were also complemented with surface remote sensing analyses from Aerosol Robotic Network (AERONET) [28].

2. Materials and Methods

2.1. Study Site and Sampling

Aerosol samples were collected at the Base Avançada de Pesquisa do Pantanal (BAPP), located 160 km south of the capital Cuiabá–MT, in the SESC Pantanal Park–Baía das Pedras (16°29′56″ S, 56°24′47″ W), in the city of Poconé (Figure 1a), and close to the SESC Private Natural Heritage Reserve (PNHR SESC). The Pantanal of Mato Grosso is located to the north of the biome, the climate is classified as Humid Tropical with rainy summers and dry winters, *Aw* in the Köppen–Geiger classification [26,27]. Climatological factors make the Pantanal a unique ecosystem, such as the flat relief and seasonal rainfall dynamics, which contribute to flooding part of the biome [21]. Considering only the cities of the Pantanal of Mato Grosso, the annual precipitation mean is approximately 1360 mm [29].

Particulate matter with an aerodynamic diameter smaller than 2.5 μm ($PM_{2.5}$) was collected using 47 mm Teflon membrane filters, which captured aerosols after the aerodynamic cut performed by the Partisol Model 2025i Sequential Air Sampler (Thermo Scientific, Waltham, MA, USA), operating at a flow rate of 17 L/min^{-1} [30,31]. The sampling system is illustrated in Figure 1b. Additionally, the system was automated, shutting down when the flow rate dropped below 16 L/min^{-1}. Due to the challenging accessibility of the collection site, each filter was sampled for 7 days or until the system automatically shut down. Each sample was placed in a Petri dish, wrapped in aluminum foil, and stored in an inert environment to prevent damage or contamination of the samples. Similar interference conditions to those described in [19], such as vehicular traffic on a nearby road, may have minimally influenced the sampling. Meanwhile, a complementary principal component analysis (PCA) [32] revealed that all emissions could be explained by a single factor, rein-

forcing that the characterization in this study pertains to $PM_{2.5}$ emissions primarily from biomass burning mixed with soil suspension. The collection campaign took place between 25 August 2022 and 14 October 2022 (2 months). Each filter represents a week average of $PM_{2.5}$ we have separated into seven analysis periods: P1 = 08/25 to 09/01, P2 = 09/02 to 09/08, P3 = 09/09 to 09/15, P4 = 09/16 to 09/22, P5 = 09/23 to 09/30, P6 = 10/01 to 10/07, and P7 = 10/08 to 10/14. The period chosen for the sampling campaign, August to October, covers the critical period of emissions for biomass burning in the study area [22,23].

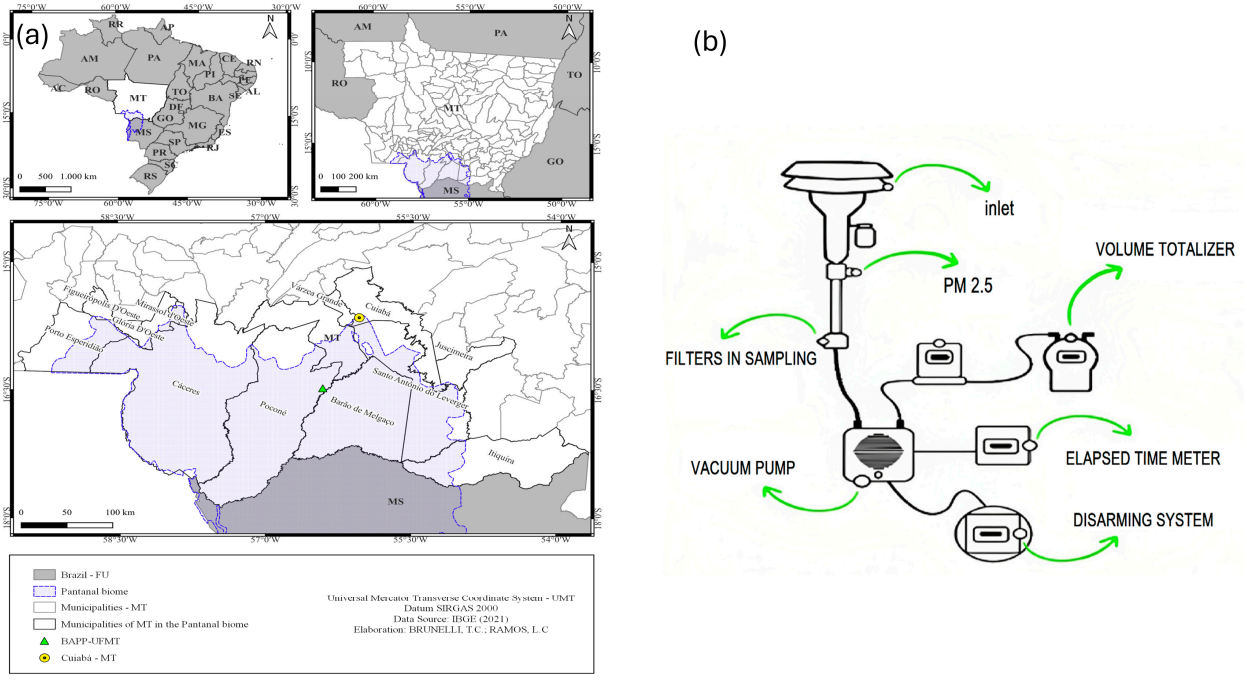

Figure 1. (**a**) Sampling site BAPP, Private Natural Heritage Reserve of SESC Pantanal–Baía das Pedras, state of Mato Grosso, north of Brazilian Pantanal, (**b**) Representation of the sampling system of atmospheric aerosol.

The samples were analyzed to determine the mass concentration of particulate matter in the atmosphere by gravimetric measurement. Before weighing, the samples had their static electricity removed by a U-shaped electrode (PRX U, Huang GmbH, Leinfelden Echterdingen, Germany). The procedure consists of determining the filter mass before and after sampling using an electronic microanalytical balance of nominal precision 1 µg (XP6U, Mettler Toledo, Greifensee, Switzerland) in a controlled environment with a temperature of 20°C and relative humidity of 50% [14]. The gravimetric method has an estimated precision of 90%, and the detection limit for the aerosol mass concentration is 0.3 µg m^{-3} [29]. The determination of BC concentration was carried out by optical reflectance analysis. The smoke stain reflectometer (M43D, Evans Electroselenium Ltd., Harlow, UK), which uses diffuse white light and a detector with a peak efficiency of around 550 nm, was calibrated with standard BC samples. The data collected from the reflectometer measures is applied to Equation (1) to determine the equivalent concentration of black carbon (BC) [33].

$$BC = [(88.3 - (77.5 \times \log R)) + (16.7 \times (\log R)^2)] \times A/V \quad (1)$$

where R is the measured reflection, A is the filter area (in this case, 13.85 cm^2), V is the volume of air in m^3, and BC concentration is given in µg m^{-3}.

Elemental analysis was performed through Energy Dispersive X-Ray Fluorescence (EDXRF) with a spectrometer (EDX-700HS, Shimadzu, Kyoto, Japan). The sample was irradiated from below with X-Rays. The fluorescence radiation is proportional to the quantity of each element, so detecting each element's energy condition allows for qualitative and quantitative analyses. The calibration of the fluorescence equipment (Epsilon 5, PANalyt-

ical, Almelo, Netherlands) can be found at [34]. Teflon filters were submitted to EDXRF, and spectra were accumulated for 900 s under the following conditions: Al filter, vacuum as X-Ray path, 10 mm diameter collimator, 10–20 keV energy range, 50 kV tube voltage, an Rh X-Ray tube, and a Si (Li) detector [35]. The analysis determined the concentration of 25 chemical elements (Na, Mg, Al, Si, P, S, Cl, K, Ca, Ti, V, Cr, Mn, Fe, Ni, Cu, Zn, As, Se, Br, Rb, Sr, Cd, Sb and Pb) in the samples. The elementary analysis made it possible to calculate the mass concentration of the Dust, according to Equation (2), where each element concentration is given in μg m^{-3} [30].

$$\text{Dust} = 1.16 \times (1.90\text{Al} + 2.15\text{Si} + 1.41\text{Ca} + 1.67\text{Ti} + 2.09\text{Fe}) \quad (2)$$

2.2. Complementary Measures and Methods

To complement the discussions, this work used records of fire outbreaks (FO) and the sum of fire radiative power (FRP) from the National Institute for Space Research, INPE over the Pantanal (available at: https://queimadas.dgi.inpe.br/queimadas/bdqueimadas (accessed on 1 September 2024)) The measurements of air temperature (Ta), relative humidity (RH), accumulated rain (AR), net radiation (Rn), and wind direction and intensity were obtained from the BAPP meteorological tower observatory. Measurements from the CUIABA-MIRANDA station of the AERONET network [28] were also used to obtain the optical depth for the fine, coarse, and total fractions of the aerosol (version 3: SDA Retrieval Level 2.0 data) [36]. The Spearman correlation was used to evaluate the relationships between $PM_{2.5}$ and BC concentrations with meteorological parameters and aerosol optical depth (AOD) values with a significance level of 95% (p-value < 0.05).

To quantify the anthropogenic influence on elemental concentrations, we adopted the enrichment factor (Ef) method, which quantifies the contribution of each element to a crustal condition [37–39] in the case of our study for background conditions. The enrichment factor (Ef) was calculated with Equation (3).

$$\text{Ef} = (\text{X}/\text{Al})_{\text{aerosol}}/(\text{X}/\text{Al})_{\text{background}} \quad (3)$$

where (X/Al) aerosol and (X/Al) background refer to the ratio between the concentration of element X for Al in the atmosphere and element X for Al in the average background mass, respectively. Al is typically used as a reference because it represents more than 8 percent of the average crustal material [37–39].

The average elemental composition for the central Amazon, as reported by Arana and Artaxo [14], was used as the background elemental composition. Elements with Ef close to 1.0 have a strong natural component while elements with high enrichment factors tend to be of artificial origin [40,41]. These reference concentrations are justified by the unique conditions of elemental concentration in the central Amazon during the rainy season. Such conditions are closer to an atmosphere as clean as in non-anthropized areas [14]. Therefore, the Ef method highlights the anthropogenic influence on the composition of atmospheric aerosols and provides a valuable parameter for gaining insights into the sources of emissions.

3. Results and Discussion

3.1. Variations in $PM_{2.5}$ and BC Concentrations

The variations in $PM_{2.5}$ concentrations for the respective analysis periods are presented in Figure 2 and detailed in Table 1. $PM_{2.5}$ concentrations ranged from approximately 7 μg m^{-3} in period P4 to more than 80 μg m^{-3} in period P5, with an overall average of 36.62 ± 31.69 μg m^{-3}. The variation value represents the standard deviation from the mean, and each individual error in PM concentration is estimated at 10%, as cited in the methods. The variations in the concentrations of black carbon (BC) and dust were also evident in Figure 2, exhibiting a similar pattern to that of $PM_{2.5}$. These results can be explained by the meteorological patterns shown in Figure 3. Although the total analysis period is classified as dry, precipitation was recorded in periods P4, P6, and P7. Figure 3A illustrates

the relationship between accumulated precipitation and aerosol load in the atmospheric column, revealing a distinct pattern of aerosol optical depth (AOD) compared to $PM_{2.5}$ measurements at the surface. The total AOD measured at 500 nm is nearly equal to the values for fine particulate matter at 500 nm (AOD_{fine}), which is characteristic of biomass burning emissions. In this case, we observe an increase in AOD from periods P1 to P4, followed by a significant reduction that reaches a minimum AOD in P6, with values close to 0.4, which are typically found during the rainy season in this region [21].

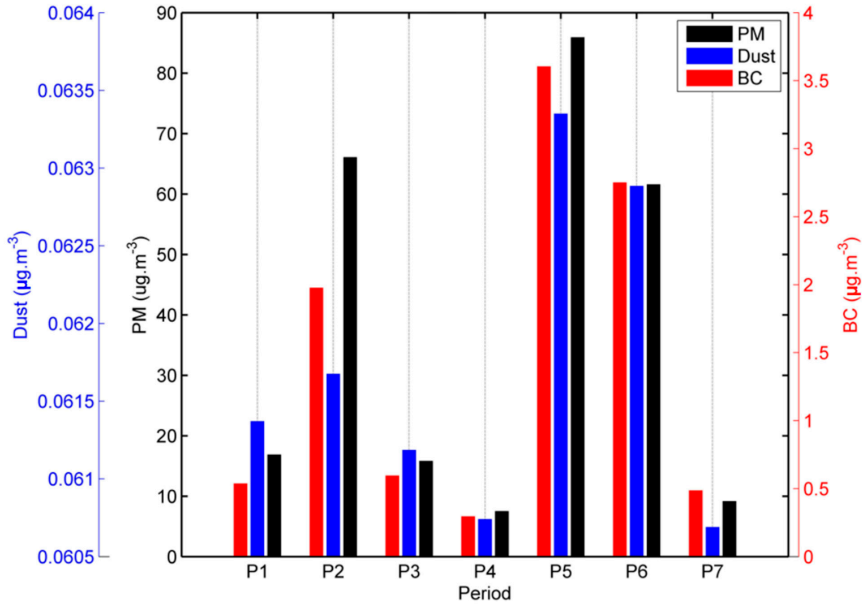

Figure 2. Concentration variation of $PM_{2.5}$, BC, and Dust concentration (µg m^{-3}) measured in the BAPP, between August and October 2022.

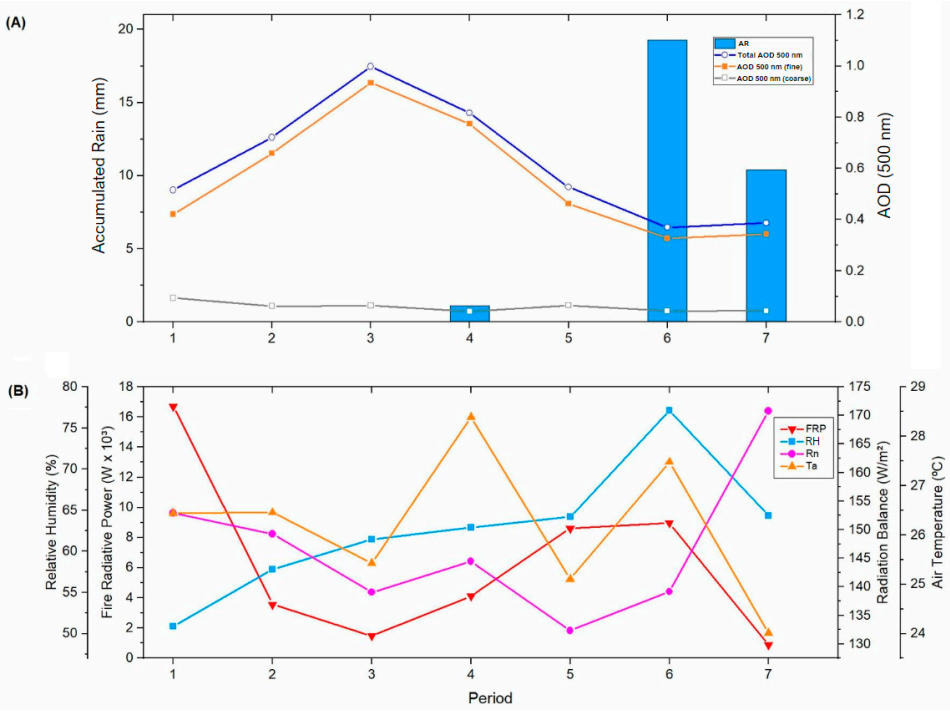

Figure 3. (**A**) Variation of Aerosol Optical Depth (AOD) 500 nm, Accumulated Rain (AR), and (**B**) meteorological conditions for the analysis period, where FRP, RH, Rn, and Ta stand for Fire Radiative Power, Relative Humidity, Net Radiation, and Air Temperature, respectively.

Table 1. Mean concentrations, standard deviations, minimums, and maximums associated with $PM_{2.5}$, BC, and elemental concentration for the entire study period ($PM_{2.5}$ and BC are expressed as μg m^{-3} and elements expressed as ng m^{-3}).

	Fine Particulate Matter BAPP Pantanal (Dry Season)			
	Mean	**Σ**	**Min**	**Max**
PM	36.62	31.69	7.02	83.66
BC	1.83	1.65	0.37	3.72
Na	94.05	95.33	19.68	279.87
Mg	28.12	27.45	0.86	81.81
Al	167.60	113.47	53.82	377.72
Si	243.52	181.99	71.59	500.15
P	33.54	38.88	5.74	98.82
S	688.32	627.43	200.90	1693.09
Cl	2.19	3.13	0.05	8.55
K	582.71	524.06	106.69	1392.17
Ca	49.07	45.44	11.56	132.15
Ti	18.93	21.01	0.02	53.30
Cr	2.05	1.71	0.42	4.62
Mn	3.86	3.30	0.74	8.65
Fe	238.28	172.63	56.47	582.40
Ni	0.53	0.49	0.11	1.45
Cu	2.65	3.15	0.69	9.16
Zn	7.66	7.22	1.33	22.49
As	0.14	0.10	0.01	0.31
Se	0.12	0.16	0.00	0.45
Br	8.62	7.47	2.36	18.84
Rb	0.98	0.80	0.20	2.53
Sr	2.27	3.96	0.00	11.00
Cd	8.56	8.48	0.85	22.37
Sb	5.47	4.55	1.78	13.39
Pb	4.28	9.16	0.08	24.93

The variation in surface concentrations has different dynamics than the aerosol load in the atmospheric column because wet deposition can act differently at each specific scale. Nevertheless, the precipitation is not enough to extinguish the burning spots, which continue to emit gases and particles that remain concentrated primarily in atmospheric regions closer to the surface. Therefore, the concentration of $PM_{2.5}$ in the dry period will directly depend on the local burning and the influences of wind intensity and direction [37,42].

At a comparative level, the work of Santos et al. [19], carried out on the same site and characterization techniques, found maximum $PM_{2.5}$ concentrations ranging from 14 to 20 μg m^{-3} during the dry period of 2012. Our results show an increase of approximately four times for the maximum concentrations of fine aerosols in the Pantanal. The work of Artaxo et al. [43], south of the Amazon biome in a region directly affected by BB emissions, found maximums varying between 300 and 350 μg m^{-3} in the 2010 drought. The study by Santanna et al. [37], with measurements close to the urban area of Cuiabá, found maximum values that varied between 50 and 60 μg m^{-3} in August 2004.

On average, $PM_{2.5}$ concentrations for the central Amazon during the dry period vary between 3.4 [43] and 4.8 μg m^{-3} [14]. For the south of the Amazon, in the arc of deforestation, this average goes to 33 μg m^{-3} [43]. The average found in our study approximates the $PM_{2.5}$ concentrations of regions highly impacted by changes in land cover due to deforestation [43,44]. It is important to note that the averages obtained in our study are based on a relatively small sample size, and these average values could shift with a higher frequency of sample collection. Nonetheless, the analyses reveal elevated concentrations of $PM_{2.5}$ during the dry period of 2022.

For BC concentrations, our results also show higher concentrations than Santos et al. [19] in the Pantanal. For the 2012 dry period, BC maximums varied between 1.6 and 1.8 μg m^{-3}, while our results show maximums of 3.7 and 2.8 μg m^{-3} in periods P5 and P6, respectively.

Recent work by Palácios et al. [21] also over the north of the Pantanal, with aethalometer measurements, found daily values above 3 μg m^{-3} for the dry periods of 2017 and 2019, years in which the Pantanal was also heavily impacted by local fires [23]. The mean for BC in our results was 1.83 ± 1.65 μg m^{-3} while Palácios et al. [21] obtained 1.01 ± 0.95, and 0.90 ± 0.81 μg m^{-3}, for the years 2017 and 2019, respectively. These differences can be justified by the differences in the methods of obtaining BC. Table 2 shows a comparison of our results for $PM_{2.5}$ and BC with other averages obtained for the Amazon in urban areas, both containing aerosol carbon sources such as biomass and fossil fuel burning.

Table 2. Comparison of means and standard deviations of $PM_{2.5}$ and BC (μg m^{-3}) for different regions in Brazil.

$PM_{2.5}$	BC	Local	Period	Reference
3.40 ± 2.00	0.23 ± 0.15	ZF2 Amazon Forest	2008–2012	Artaxo et al. [43]
33.00 ± 36.00	2.80 ± 2.92	PVH Amazon deforested	2009–2012	Artaxo et al. [43]
1.65 ± 0.92	0.09 ± 0.06	ZF2 Amazon Forest	2008	Arana and Artaxo [14]
7.60 ± 3.70	1.20 ± 0.80	Cuiabá	2004	Santanna et al. [37]
26.72 ± 14.20	2.27 ± 1.30	São Paulo	2019	Vieira et al. [35]
8.66 ± 3.14	0.76 ± 0.42	Pantanal	2012	Santos et al. [19]
--	0.75 ± 0.83	Pantanal	2017–2019	Palácios et al. [21]
36.62 ± 31.69	1.83 ± 1.65	Pantanal	2022	This work

All information in Table 2 was extracted for the fine fraction of aerosols in the period considered dry, that is, with the influences of BB emissions. The results show large variations between $PM_{2.5}$ and BC values which can be explained by several factors, such as the acquiring method, characteristic local emission, and the sampling period. Regarding the sampling period, we highlight that for El Niño years, the central and northern regions of Brazil are influenced by a precipitation deficit, causing an increase in the dry period resulting in larger burned areas and more emissions of aerosols. The study by Palácios et al. [42] showed that for El Niño conditions, there is a significant increase in the aerosol load south of the Amazon basin. The increase in BC concentrations found in this study may have a direct influence on the local microclimate, giving positive feedback on temperature maximums [10]. The study by Curado et al. [45] in the Pantanal showed a positive correlation between BC and temperature maximums with consequences for carbon capture.

3.2. Meteorological Influences

Figure 3 shows the average meteorological conditions for each period of analysis. Although there is no direct relationship, it is possible to observe some relationships between AOD_{total}, $PM_{2.5}$, and BC concentrations. AOD_{total} values were above 0.4 in the initial five periods and the third period presented the highest AOD_{fine} average, 0.93. We emphasize that the AOD_{fine} is linked to the amount of fine optically active aerosols in the atmosphere, therefore a good correlation with $PM_{2.5}$ is expected. However, differences in the observed patterns emerged across the analyzed periods. Between P1 and P2, AOD_{fine} and $PM_{2.5}$ exhibited similar behaviors. In the P3 onward, surface concentrations decreased while AOD_{fine} continued to increase. The patterns of air temperature and relative humidity mirrored the surface measurements [44]. Air temperature gradually increased from P1 to P2 before declining in P3. These findings are consistent with the positive correlation between BC concentration and maximum air temperature.

Figure 3B also shows the average behavior of the Rn. The behavior of Rn has no relationship with AOD_{total} or surface concentrations because this interaction is complex [44,46]. Blocking direct solar radiation, through scattering or absorption, can negatively influence Rn, however, retention of this radiation in the atmosphere can increase the amount of long-wave radiation, influencing Rn positively [45,47]. In general, more measurements in a specific experimental design need to be developed in the Pantanal so that these feedback processes are better understood. In this study, we justify the main variations in surface

concentrations based on the number of burning spots that occurred during the analysis period. Fire Outbreaks (FO) is a recurring problem in the Pantanal due to the environmental impact and the damage to health they can cause [22,48]. During the dry season, fires are constant as shown in Figure 4, and with the contribution of wind intensity and direction (Figure 5), concentrations can still increase due to transport in the atmosphere [21].

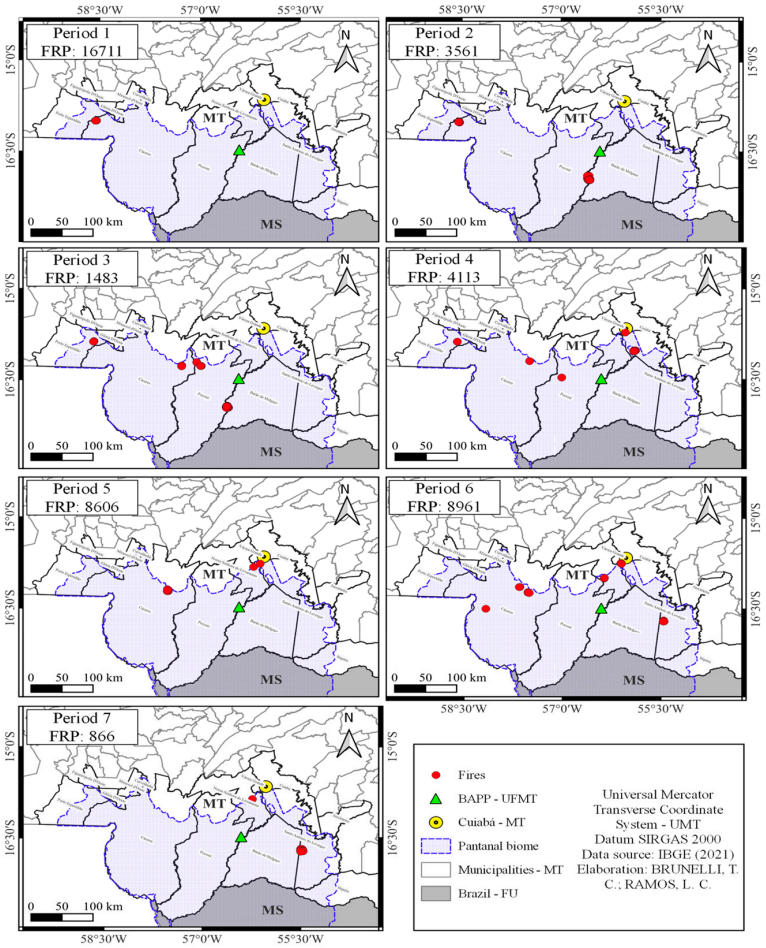

Figure 4. Geographical distribution of fires by period in the municipalities of Mato Grosso in the Pantanal biome between August and October 2022.

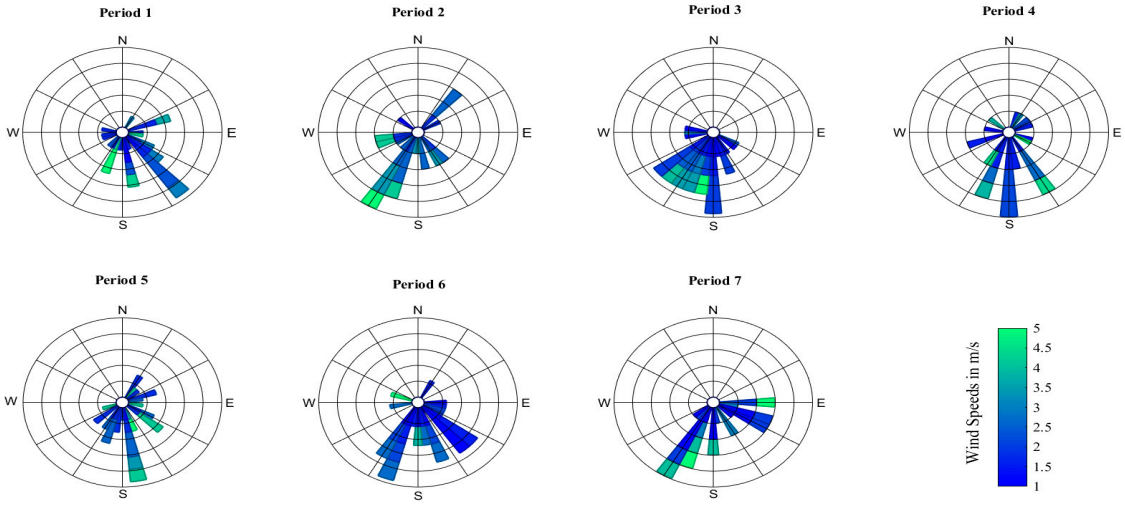

Figure 5. Roses of wind indicating the mean velocity and direction of the wind throughout the period between August and October 2022 measured at the micrometeorological tower in the BAPP.

Our analysis shows that P1 obtained the highest value for FRP, reaching 16,711 W, however, the distance from BAPP, FO (Figure 4), wind direction (Figure 5), and $PM_{2.5}$ concentration (Figure 2) suggest low BB influence on collected samples. The largest $PM_{2.5}$ peaks occur in the second, fifth, and sixth periods, with the values of FRP 3561, 8606, and 8961 W, respectively. Considering the position of the FO and the wind speed and direction, the samples collected in these periods may have been directly influenced by regional forest fires. Furthermore, period five (P5) presented the highest number of FO (Figure 4) and at the same time the maximum dust concentration of 3.7 μg m^{-3} (Figure 2). When analyzing the correlations between surface concentrations ($PM_{2.5}$ and BC) with the other variables used in this study, no statistically significant correlation was found. The similarity in the variation of black carbon (BC) and dust concentrations suggests that aerosol composition in the northern Pantanal during the dry season is a mixture of biomass burning and soil resuspension. The PCA analysis confirmed that 99% of the emissions could be explained by a single factor.

In addition, the wind intensity contributes to soil suspension. Crossed with other factors such as land use and models of particle dispersion, it determines some aspects of aerosol composition and their trajectory [36,49], however, this work is focused on the characterization of $PM_{2.5}$, thus a qualitative analysis of air conditions and elemental concentration was enough. Despite this, the spatial and temporal variability of aerosols over a long 1 week must influence the correlation between $PM_{2.5}$ concentrations and the other meteorological variables. Precipitation events should decrease the concentration of PM in the atmosphere [50], such as the variation observed in P6 to P7. Nonetheless, the continuous emissions of biomass and soil suspension could rapidly increase the concentrations of $PM_{2.5}$, BC, and Dust.

3.3. Elemental Concentration and Enrichment Factor

Figure 6 presents the most significant elemental concentrations observed during the study period. In comparison with the study by Santos et al. [19], an increase in the concentrations of sulfur (S), potassium (K), iron (Fe), and silicon (Si) is noticeable. While the concentrations of Fe and Si are close to those measured in 2012, the maximum concentrations of S and K were three times higher. Elemental concentrations follow the same pattern as $PM_{2.5}$ and BC concentrations with small variations for Si and Fe. For Si, concentrations were the same in periods P5 and P6, while Fe suffered an approximate reduction of 50% for the respective periods. The study by Santanna et al. [37] explains that the increased concentrations of aluminum (Al), silicon (Si), and iron (Fe) during the dry season are primarily linked to soil conditions, as these elements are characteristic of crustal material and among the most abundant in Earth's crust. During this period, arid soil, combined with higher average wind speeds and minimal precipitation, transforms the soil into a significant emission source, contributing to aerosol levels alongside biomass burning.

Although the factor analysis was limited by the sample quantity, the dominant elemental concentrations still show a strong association with biomass burning emissions, with additional contributions from soil resuspension [14,19,37,42]. In fact, 99% of the emissions were attributed to a single factor that we identify as a mixture between BC and Dust. The concentrations of Fe, S, and K can be a good indication of BB contribution. The classic study by Andreae [51] highlights that the concentrations of K can be used as an indicator of fires in the flaming phase. However, Urban et al. [52] highlight the limitations of using K as a marker when studying soil resuspension emissions in fertilized areas.

For the heavy metals Pb and Cd, the averages found in our study were 4.28 and 8.56 ng m^{-3}. In the case of Pb, the maximum concentration reached 24.93 ng m^{-3}. This peak value occurred in P5, and is six times higher than the average concentration for this element (see Table 1). The presence of Pb may be related to anthropogenic factors, especially mining activities that contaminate the soil with heavy metals and increase the suspension of contaminated soil [52]. The dust compound, calculated from the concentration of the elements Al, Si, Ca, Ti, and Fe (Equation (2)), is the main constituent of natural atmospheric

aerosols. Annually, the Amazon receives a substantial load of dust from the African continent, which transports tons across the Pacific Ocean [43,49]. In the Pantanal, land use by agricultural activities, mining, and vehicle traffic is responsible for the suspension of dust, which, depending on the composition of the soil, can pose health risks [19,53]. This work calculated the maximum dust concentration at 3.7 μg m^{-3}, while in the study by Morais [33] during the dry season at the Amazon Tall Tower Observatory (ATTO), the maximum concentration was 1.4 μg m^{-3}, highlighting that areas with greater concentration of human activities promote greater soil suspension.

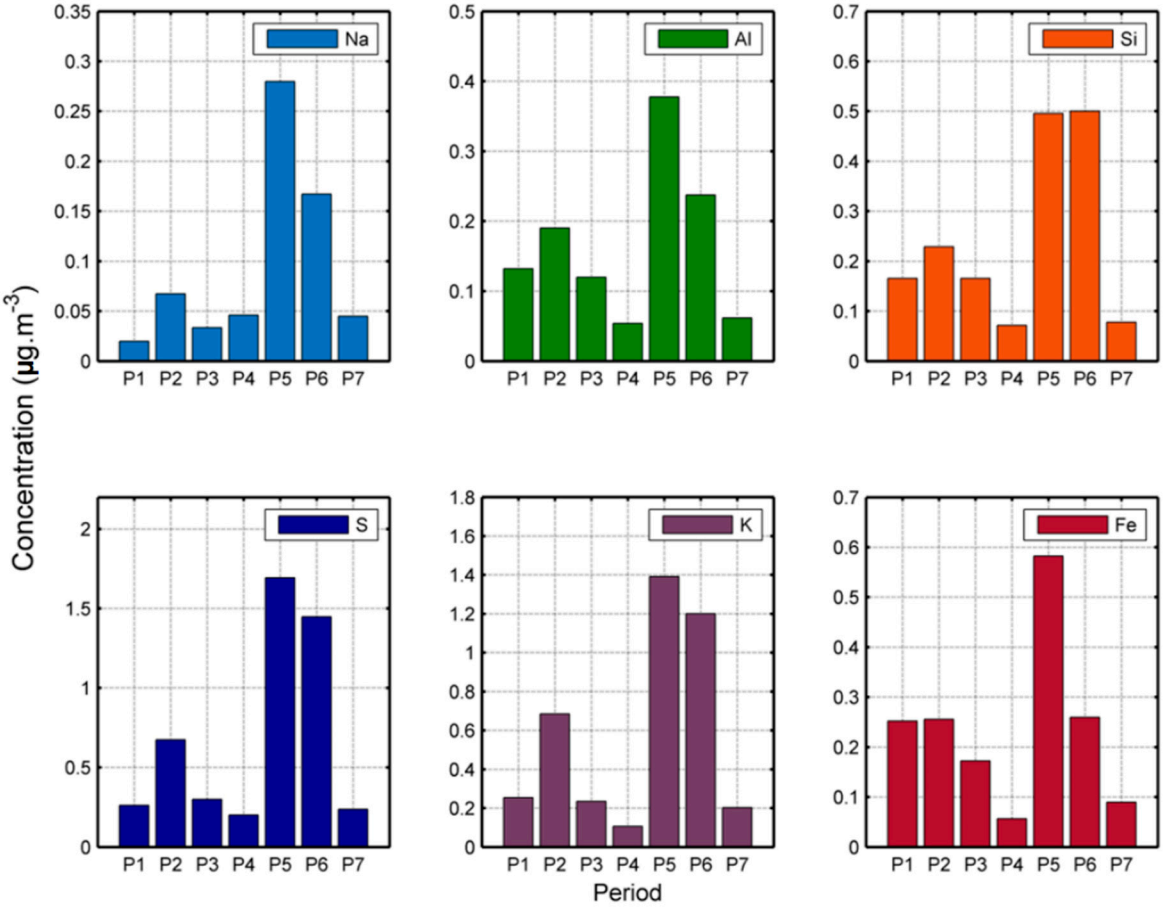

Figure 6. Variation in the mean concentration of major chemical elements during the study period.

Reference measurements from Arana and Artaxo [14] facilitated the determination of the enrichment factor (Ef) for 17 elements, as illustrated in Figure 7. The results in Figure 7 show that for all evaluated elements, there is an anthropogenic contribution. For the fine fraction of aerosols, BB emissions are responsible for the high values of K, S, Mg, and Zn [29,54]. In this case, we highlight the Ef of K which was approximately 10 times higher than the natural concentration. As for soil resuspension emissions, we have increases in Al, Si, Ti, Fe, Ni, and Cu, which varied in elevations of 1.6 for Si and 12.8 for Cu (times higher). The results also show that Pb was the most anthropic contribution element in the study with Ef above 200 times the natural emission value, although its average concentration is low (see Table 1). The results identified in this study are generally consistent with those obtained by Santanna et al. [37], although the values are approximately 10 times higher for most elements. The concentrations of Cl, K, and Br can be attributed to biomass burning, while Fe, Cu, Zn, and Pb suggest anthropogenic emissions. This indicates that the region is undergoing significant anthropogenic transformation, which may have serious implications for the environment and public health. As previously mentioned, these transformations can

be directly associated with mining activities that contaminate the soil with heavy metals and increase the suspension of contaminated soil [49].

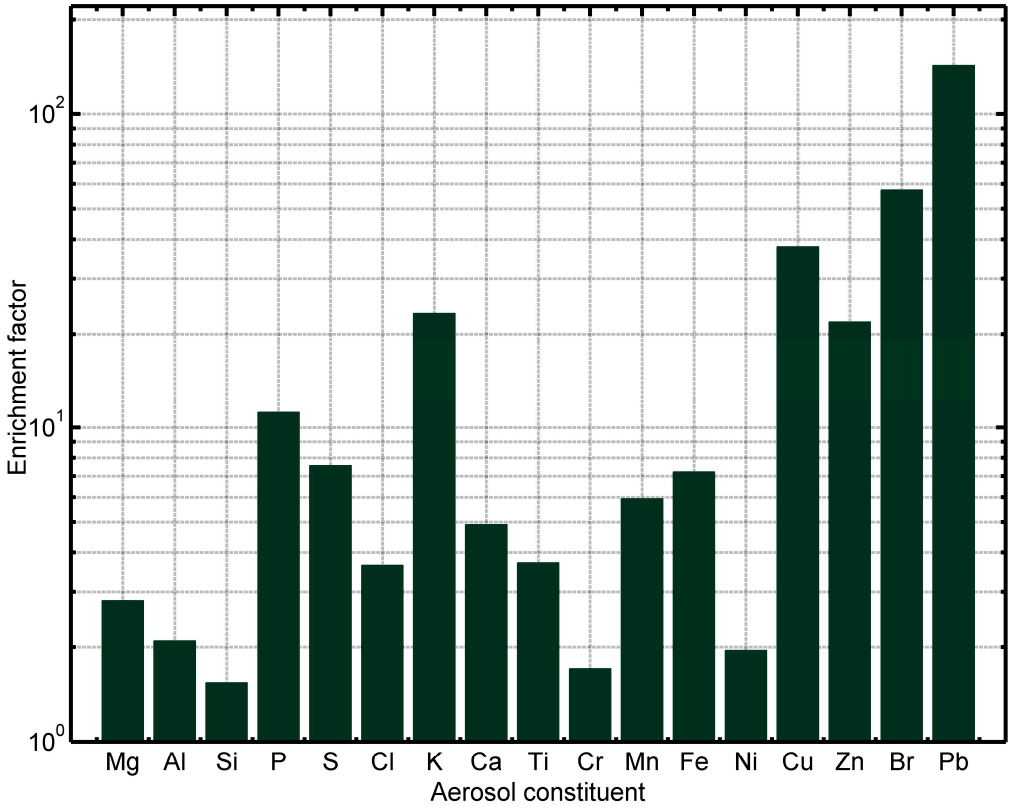

Figure 7. Enrichment factors (Ef) for the $PM_{2.5}$ fraction. Enrichment factors close to 1 indicate a natural source while enrichment factors > 1 indicate an anthropogenic source.

4. Conclusions

In this study, the mass concentrations of $PM_{2.5}$ and BC were determined through gravimetric analysis and optical reflectance during the dry period of 2022 in the northern Pantanal. Concentrations varied across the analyzed periods, reflecting local BB emissions. The average concentration of $PM_{2.5}$ was 36.62 ± 31.69 μg m^{-3}, while BC had an average of 1.83 ± 1.65 μg m^{-3}. These concentrations represent increases of approximately 80% and 60% for $PM_{2.5}$ and BC, respectively, compared to those recorded a decade ago at the same site. The elemental concentration of S, K, Fe, and Si has also increased significantly in the last decade. In this study, the concentration of those elements reached 688.32 ± 627.43, 582.71 ± 524.06, 238.28 ± 172.63, and 243.52 ± 181.99 ng m^{-3}, respectively. Additionally, other elements such as Pb, with a maximum concentration of 24.93 ng m^{-3}, and Cd, with a maximum concentration of 22.37 ng m^{-3} indicate a worrying concentration. Furthermore, a significant increase in heavy metals was found in the composition of aerosols. Notably, the average concentration of Pb, which was the most significant constituent in the enrichment analysis, exhibited values 200 greater than those typically observed under clear atmospheric conditions. We also emphasized the enrichment factor values for Br and Cu. These compounds indicate a strong anthropogenic contribution, primarily emitted by biomass burning and gold mining. Environmental factors such as wind speed and low precipitation values contribute to soil suspension as an aerosol source, indicating that aerosols emitted in the dry season period are predominantly a mix of biomass burning and dust. The results, both in terms of elemental composition and BC concentration over the 10-year interval, indicate a shift in the regional dynamics of the Pantanal. We suspect that the increase in anthropogenic activities in the biome in the last decade is responsible for this change in the

concentration and composition of atmospheric aerosols in the Pantanal Mato Grosso and we aim to explore this issue further in future research.

Author Contributions: Conceptualization, L.C.R., J.B.M. and F.C.V.; Methodology, L.C.R. and T.C.B.; software, T.C.B. and J.B.M.; Validation, F.C.V., R.d.S.P. and A.M.d.S.L.; Investigation, L.C.R., F.G.M., J.B.M. and F.C.V.; Resources, J.B.M. and L.F.A.C.; Data curation, L.C.R., R.d.S.P. and F.G.M.; writing—original draft preparation, L.C.R. and T.C.B.; writing—review and editing, N.N.d.O., F.G.M., A.M.d.S.L., L.F.A.C. and F.C.V. All authors have read and agreed to the published version of the manuscript.

Funding: The research was funded by Coordenação de Aperfeiçoamento de Pessoal de Nível Superior (CAPES). The authors thank the concession of research grant processes (88887.625975/2021-00 and 88887.496169/2020-00).

Institutional Review Board Statement: Not applicable.

Informed Consent Statement: Not applicable.

Data Availability Statement: The AERONET website provides data analysis and dissemination tools at https://aeronet.gsfc.nasa.gov (accessed on 16 November 2022). Data can be viewed in the data display interface, acquired using the data download tool, analyzed, and downloaded using some analysis tools provided by AERONET. The INPE website provides data analysis and dissemination tools at https://queimadas.dgi.inpe.br/queimadas/portal (accessed on 20 November 2022). Every other data must be requested directly from the authors.

Acknowledgments: The authors appreciate P. Artaxo and J. S. Nogueira, as well as their team, for establishing and maintaining the site used in the investigation; the members of Laboratório de Física Atmosférica (LFA–USP) for supporting in the samples analyses; and Pró-Reitoria de Pesquisa e Pós-graduação da Universidade Federal de Mato Grosso PROPG/UFMT.

Conflicts of Interest: The authors declare no conflicts of interest.

References

1. *IPCC AR5 Climate Change 2013: The Physical Science Basis*; IPCC: Geneva, Switzerland, 2013; Volume 92, ISBN 9781107415324.
2. Kumar, M.; Raju, M.P.; Singh, R.S.; Banerjee, T. Impact of Drought and Normal Monsoon Scenarios on Aerosol Induced Radiative Forcing and Atmospheric Heating in Varanasi over Middle Indo-Gangetic Plain. *J. Aerosol Sci.* **2017**, *113*, 95–107. [CrossRef]
3. Kumar, K.R.; Sivakumar, V.; Yin, Y.; Reddy, R.R.; Kang, N.; Diao, Y.; Adesina, A.J.; Yu, X. Long-Term (2003–2013) Climatological Trends and Variations in Aerosol Optical Parameters Retrieved from MODIS over Three Stations in South Africa. *Atmos. Environ.* **2014**, *95*, 400–408. [CrossRef]
4. Kang, N.; Kumar, K.R.; Hu, K.; Yu, X.; Yin, Y. Long-Term (2002–2014) Evolution and Trend in Collection 5.1 Level-2 Aerosol Products Derived from the MODIS and MISR Sensors over the Chinese Yangtze River Delta. *Atmos. Res.* **2016**, *181*, 29–43. [CrossRef]
5. Rizzo, L.V.; Artaxo, P.; Müller, T.; Wiedensohler, A.; Paixão, M.; Cirino, G.G.; Arana, A.; Swietlicki, E.; Roldin, P.; Fors, E.O.; et al. Long Term Measurements of Aerosol Optical Properties at a Primary Forest Site in Amazonia. *Atmos. Chem. Phys.* **2013**, *13*, 2391–2413. [CrossRef]
6. Thornhill, G.D.; Ryder, C.L.; Highwood, E.J.; Shaffrey, L.C.; Johnson, B.T. The Effect of South American Biomass Burning Aerosol Emissions on the Regional Climate. *Atmos. Chem. Phys.* **2018**, *18*, 5321–5342. [CrossRef]
7. Bond, T.C.; Doherty, S.J.; Fahey, D.W.; Forster, P.M.; Berntsen, T.; Deangelo, B.J.; Flanner, M.G.; Ghan, S.; Kärcher, B.; Koch, D.; et al. Bounding the Role of Black Carbon in the Climate System: A Scientific Assessment. *J. Geophys. Res. Atmos.* **2013**, *118*, 5380–5552. [CrossRef]
8. Bennett, J.E.; Tamura-Wicks, H.; Parks, R.M.; Burnett, R.T.; Pope, C.A.; Bechle, M.J.; Marshall, J.D.; Danaei, G.; Ezzati, M. Particulate Matter Air Pollution and National and County Life Expectancy Loss in the USA: A Spatiotemporal Analysis. *PLoS Med.* **2019**, *16*, 1002856. [CrossRef]
9. Requia, W.J.; Amini, H.; Mukherjee, R.; Gold, D.R.; Schwartz, J.D. Health Impacts of Wildfire-Related Air Pollution in Brazil: A Nationwide Study of More than 2 Million Hospital Admissions between 2008 and 2018. *Nat. Commun.* **2021**, *12*, 6555. [CrossRef]
10. IPCC. *Climate Change 2022: Impacts, Adaptation, and Vulnerability. Contribution of Working Group II to the Sixth Assessment Report of the Intergovernmental Panel on Climate Change*; IPCC: Cambridge, UK, 2022.
11. de Andrade Filho, V.S.; Artaxo, P.; Hacon, S.; do Carmo, C.N.; Cirino, G. Aerossois de Queimadas e Doencas Respiratorias em Criancas, Manaus, Brasil. *Rev. Saude Publica* **2013**, *47*, 239–247. [CrossRef]
12. Brunelli, T.C.; Paiva, S.; Yara, A.; Elizeu, C.; Otávio, L.; Basso, J. Environmental parameters and relationships with COVID-19 cases in central South America. *Quim. Nova* **2021**, *44*, 1236–1244. [CrossRef]
13. Jacobson, L.d.S.V.; de Oliveira, B.F.A.; Schneider, R.; Gasparrini, A.; Hacon, S.d.S. Mortality Risk from Respiratory Diseases Due to Non-Optimal Temperature among Brazilian Elderlies. *Int. J. Environ. Res. Public Health* **2021**, *18*, 5550. [CrossRef] [PubMed]

14. Arana, A.; Artaxo, P. Composição Elementar do Aerossol Atmosférico na Região Central da Bacia Amazônica. *Quim. Nova* **2014**, *37*, 268–276. [CrossRef]
15. Rizzo, L.V.; Correia, A.L.; Artaxo, P.; Procápio, A.S.; Andreae, M.O. Spectral Dependence of Aerosol Light Absorption over the Amazon Basin. *Atmos. Chem. Phys.* **2011**, *11*, 8899–8912. [CrossRef]
16. Rizzo, L.V.; Roldin, P.; Brito, J.; Backman, J.; Swietlicki, E.; Krejci, R.; Tunved, P.; Petäjä, T.; Kulmala, M.; Artaxo, P. Multi-Year Statistical and Modeling Analysis of Submicrometer Aerosol Number Size Distributions at a Rain Forest Site in Amazonia. *Atmos. Chem. Phys.* **2018**, *18*, 10255–10274. [CrossRef]
17. Saturno, J.; Holanda, B.A.; Pöhlker, C.; Ditas, F.; Wang, Q.; Moran-Zuloaga, D.; Brito, J.; Carbone, S.; Cheng, Y.; Chi, X.; et al. Black and Brown Carbon over Central Amazonia: Long-Term Aerosol Measurements at the ATTO Site. *Atmos. Chem. Phys.* **2018**, *18*, 12817–12843. [CrossRef]
18. Ponczek, M.; Franco, M.A.; Carbone, S.; Rizzo, L.V.; Monteiro dos Santos, D.; Morais, F.G.; Duarte, A.; Barbosa, H.M.J.; Artaxo, P. Linking the Chemical Composition and Optical Properties of Biomass Burning Aerosols in Amazonia. *Environ. Sci. Atmos.* **2021**, *2*, 252–269. [CrossRef]
19. Santos, A.C.A.; Finger, A.; De Souza Nogueira, J.; Curado, L.F.A.; Da Silva Palácios, R.; Pereira, V.M.R. Análise Da Concentração e Composição de Aerossóis de Queimadas do Pantanal Mato-Grosso. *Quim. Nova* **2016**, *39*, 919–924. [CrossRef]
20. Marengo, J.A.; Cunha, A.P.; Cuartas, L.A.; Deusdará Leal, K.R.; Broedel, E.; Seluchi, M.E.; Michelin, C.M.; De Praga Baião, C.F.; Chuchón Ângulo, E.; Almeida, E.K.; et al. Extreme Drought in the Brazilian Pantanal in 2019–2020: Characterization, Causes, and Impacts. *Front. Water* **2021**, *3*, 639204. [CrossRef]
21. Palácios, R.; Romera, K.; Rizzo, L.; Cirino, G.; Adams, D.; Imbiriba, B.; Nassarden, D.; Rothmund, L.; Siqueira, A.; Basso, J.; et al. Optical Properties and Spectral Dependence of Aerosol Light Absorption over the Brazilian Pantanal. *Atmos. Pollut. Res.* **2022**, *13*, 101413. [CrossRef]
22. Libonati, R.; Geirinhas, J.o.L.; Silva, P.S.; Russo, A.; Rodrigues, J.A.; Belém, L.B.C.; Nogueira, J.; Roque, F.O.; Dacamara, C.C.; Nunes, A.M.B.; et al. Assessing the Role of Compound Drought and Heatwave Events on Unprecedented 2020 Wildfires in the Pantanal. *Environ. Res. Lett.* **2022**, *17*, 015005. [CrossRef]
23. Garcia, L.C.; Szabo, J.K.; de Oliveira Roque, F.; de Matos Martins Pereira, A.; Nunes da Cunha, C.; Damasceno-Júnior, G.A.; Morato, R.G.; Tomas, W.M.; Libonati, R.; Ribeiro, D.B. Record-Breaking Wildfires in the World's Largest Continuous Tropical Wetland: Integrative Fire Management Is Urgently Needed for Both Biodiversity and Humans. *J. Environ. Manag.* **2021**, *293*, 112870. [CrossRef] [PubMed]
24. Kumar, S.; Getirana, A.; Libonati, R.; Hain, C.; Mahanama, S.; Andela, N. Changes in Land Use Enhance the Sensitivity of Tropical Ecosystems to Fire-Climate Extremes. *Sci. Rep.* **2022**, *12*, 964. [CrossRef]
25. Martins, P.I.; Belém, L.B.C.; Szabo, J.K.; Libonati, R.; Garcia, L.C. Prioritising Areas for Wildfire Prevention and Post-Fire Restoration in the Brazilian Pantanal. *Ecol. Eng.* **2022**, *176*, 106517. [CrossRef]
26. Köppen, G.W.; Geiger, M.R. *Handbuch Der Klimatologie*; Salzwasser: Berlin, Germany, 1936.
27. Guimarães, D.P.; Landau, E.C.; Santos, M.C.B.; Mendes, S.H.G.d.S. *Caracterização de Chuvas do Pantanal Mato-Grossense*; Embrapa: Brasilia, Brasil, 2018; Volume 15.
28. Holben, B.N.; Eck, T.F.; Slutsker, I.; Tanré, D.; Buis, J.P.; Setzer, A.; Vermote, E.; Reagan, J.A.; Kaufman, Y.J.; Nakajima, T.; et al. AERONET—A Federated Instrument Network and Data Archive for Aerosol Characterization. *Remote Sens. Environ.* **1998**, *66*, 1–16. [CrossRef]
29. Artaxo, P.; Martins, J.V.; Yamasoe, M.A.; Procópio, A.S.; Pauliquevis, T.M.; Andreae, M.O.; Guyon, P.; Gatti, L.V.; Leal, A.M.C. Physical and Chemical Properties of Aerosols in the Wet and Dry Seasons in Rondônia, Amazonia. *J. Geophys. Res. Atmos.* **2002**, *107*, LBA 49-1–LBA 49-14. [CrossRef]
30. Maenhaut, W.; Raes, N.; Chi, X.; Cafmeyer, J.; Wang, W.; Salma, I. Chemical Composition and Mass Closure for Fine and Coarse Aerosols at a Kerbside in Budapest, Hungary, in Spring 2002. *X-Ray Spectrom.* **2005**, *34*, 290–296. [CrossRef]
31. Mcmurry, P.H. A Review of Atmospheric Aerosol Measurements. *Atmos. Environ.* **2000**, *34*, 1959–1999. [CrossRef]
32. Veltkamp, P.R.; Hansen, K.J.; Barkley, R.M.; Sievers, R.E. Principal Component Analysis of Summertime Organic Aerosols at Niwot Ridge, Colorado. *JGR Atmos.* **1996**, *101*, 495–504. [CrossRef]
33. Morais, F.G. *Estudo das Propriedades de Absorção de Brown Carbon e Black Carbon Utilizando Sensoriamento Remoto e Medidas In Situ Na Amazônia*; Instituto de Pesquisas Energéticas e Nucleares: Sao Paolo, Brasil, 2022.
34. Arana, A.A. Aerossóis Atmosféricos Na Amazônia: Composição Orgânica e Inorgânica em Regiões Com Diferentes Usos do Solo. Ph.D. Thesis, Universidade Estadual do Amazonas, Manaus, Brasil, 2014.
35. Vieira, E.V.R.; do Rosario, N.E.; Yamasoe, M.A.; Morais, F.G.; Martinez, P.J.P.; Landulfo, E.; Maura de Miranda, R. Chemical Characterization and Optical Properties of the Aerosol in São Paulo, Brazil. *Atmosphere* **2023**, *14*, 1460. [CrossRef]
36. Sena, E.T.; Artaxo, P.; Correia, A.L. Spatial Variability of the Direct Radiative Forcing of Biomass Burning Aerosols and the Effects of Land Use Change in Amazonia. *Atmos. Chem. Phys.* **2013**, *13*, 1261–1275. [CrossRef]
37. Santanna, F.B.; De Almeida Filho, E.O.; Vourlitis, G.L.; De Arruda, P.H.Z.; Da Silva Palácios, R.; De Souza Nogueira, J. Elemental Composition of PM10 and PM2.5 for A Savanna (Cerrado) Region of Southern Amazonia. *Quim. Nova* **2016**, *39*, 1170–1176. [CrossRef]
38. Duce, R.A.; Hoffman, G.L.; Zoller, W.H. Atmospheric Trace Metals at Remote Northern and Southern Hemisphere Sites: Pollution or Natural? *Science* **1975**, *187*, 59–61. [CrossRef] [PubMed]

39. Zoller, W.H.; Duce, E.S. Atmospheric Concentrations and Sources of Trace Metals at the South Pole. *Science* **1974**, *183*, 198–200. [CrossRef] [PubMed]
40. Marcazzan, G.M.; Vaccaro, S.; Valli, G.; Vecchi, R. Characterisation of PM10 and PM2.5 Particulate Matter in the Ambient Air of Milan (Italy). *Atmos. Environ.* **2001**, *35*, 4639–4650. [CrossRef]
41. Braga, C.F.; Teixeira, E.C.; Meira, L.; Wiegand, F.; Yoneama, M.L.; Dias, J.F. Elemental Composition of PM10 and PM2.5 in Urban Environment in South Brazil. *Atmos. Environ.* **2005**, *39*, 1801–1815. [CrossRef]
42. Artaxo, P.; Rizzo, L.V.; Brito, J.F.; Barbosa, H.M.J.; Arana, A.; Sena, E.T.; Cirino, G.G.; Bastos, W.; Martin, S.T.; Andreae, M.O. Atmospheric Aerosols in Amazonia and Land Use Change: From Natural Biogenic to Biomass Burning Conditions. *Faraday Discuss.* **2013**, *165*, 203–235. [CrossRef]
43. Palácios, R.d.S.; Romera, K.S.; Curado, L.F.A.; Banga, N.M.; Rothmund, L.D.; Sallo, F.d.S.; Morais, D.; Santos, A.C.A.; Moraes, T.J.; Morais, F.G.; et al. Long Term Analysis of Optical and Radiative Properties of Aerosols in the Amazon Basin. *Aerosol Air Qual. Res.* **2020**, *20*, 139–154. [CrossRef]
44. Palácios, R.; Castagna, D.; Barbosa, L.; Souza, A.P.; Imbiriba, B.; Zolin, C.A.; Nassarden, D.; Duarte, L.; Morais, F.G.; Franco, M.A.; et al. ENSO Effects on the Relationship between Aerosols and Evapotranspiration in the South of the Amazon Biome. *Environ. Res.* **2024**, *250*, 118516. [CrossRef]
45. Curado, L.F.A.; de Paulo, S.R.; da Silva, H.J.A.; Palácios, R.S.; Marques, J.B.; de Paulo, I.J.C.; Dalmagro, H.J.; Rodrigues, T.R. Effect of Biomass Burning Emission on Carbon Assimilation over Brazilian Pantanal. *Theor. Appl. Climatol.* **2024**, *155*, 999–1006. [CrossRef]
46. Huang, Y.; Mahrt, F.; Xu, S.; Shiraiwa, M.; Zuend, A.; Bertram, A.K. Coexistence of Three Liquid Phases in Individual Atmospheric Aerosol Particles. *Proc. Natl. Acad. Sci. USA* **2021**, *118*, e2102512118. [CrossRef]
47. Palancar, G.G.; Olcese, L.E.; Lanzaco, B.L.; Achad, M.; López, M.L.; Toselli, B.M. Aerosol Radiative Forcing Efficiency in the UV-B Region over Central Argentina. *Atmos. Res.* **2016**, *176–177*, 1–9. [CrossRef]
48. Caumo, S.; Lázaro, W.L.; Sobreira Oliveira, E.; Beringui, K.; Gioda, A.; Massone, C.G.; Carreira, R.; de Freitas, D.S.; Ignacio, A.R.A.; Hacon, S. Human Risk Assessment of Ash Soil after 2020 Wildfires in Pantanal Biome (Brazil). *Air Qual. Atmos. Health* **2022**, *15*, 2239–2254. [CrossRef] [PubMed]
49. Garba, S.; Abubakar, M. Source and Distribution of The Heavy Metals: Pb, Cd, Cu, Zn, Fe, Cr, and Mn in Soils of Bauchi Metropolis, Nigeria. *Am. J. Eng. Res.* **2018**, *7*, 13–22.
50. Possanzini, M.; Buttini, P.; Di Palo, V. Characterization of a Rural Area in Terms of Dry and Wet Deposition. *Sci. Total Environ.* **1988**, *74*, 111–120. [CrossRef]
51. Andreae, M.A. Soot Carbon and Excess Fine Potassium: Long-Range Transport of Combustion-Derived Aerosols. *Science* **1983**, *220*, 1148–1151. [CrossRef] [PubMed]
52. Urban, R.C.; Lima-Souza, M.; Caetano-Silva, L.; Queiroz, M.E.C.; Nogueira, R.F.P.; Allen, A.G.; Cardoso, A.A.; Held, G.; Campos, M.L.A.M. Use of Levoglucosan, Potassium, and Water-Soluble Organic Carbon to Characterize the Origins of Biomass-Burning Aerosols. *Atmos. Environ.* **2012**, *61*, 562–569. [CrossRef]
53. Caumo, S.; Yera, A.B.; Vicente, A.; Alves, C.; Roubicek, D.A.; de Castro Vasconcellos, P. Particulate Matter–Bound Organic Compounds: Levels, Mutagenicity, and Health Risks. *Environ. Sci. Pollut. Res.* **2022**, *29*, 31293–31310. [CrossRef] [PubMed]
54. Reid, J.S.; Hobbs, P.V.; Ferek, R.J.; Blake, D.R.; Martins, J.V.; Dunlap, M.R.; Liousse, C. Physical, Chemical, and Optical Properties of Regional Hazes Dominated by Smoke in Brazil. *J. Geophys. Res. Atmos.* **1998**, *103*, 32059–32080. [CrossRef]